Progress In Electromagnetics Research C, Vol. 136, 1–12, 2023

A Novel Metamaterial-Inspired UWB and ISM Multiband Antenna for Wireless Communications: Design and Characteristic Mode Analysis

Leila Ghanbari*, Asghar Keshtkar, and Saughar Jarchi

Abstract—This article introduces a new planar multiband antenna inspired by metamaterials. The design incorporates a split-ring resonator (SRR) on a printed monopole antenna for ultra-wideband (UWB) communication, generating a new resonant frequency within the Industrial, Scientific, and Medical (ISM) frequency band. The effect of SRR-inspired slots was examined using characteristic mode analysis (CMA), revealing that the placement of the SRR on the antenna's radiating structure created multiple resonant modes. To improve impedance matching, the ground plane of the antenna was modified. The antenna was fed using a 50 Ω microstrip line. The proposed antenna was simulated and fabricated on an inexpensive FR4 substrate with a thickness of 1.6 mm, a dielectric constant of 4.4, and dimensions of $38 \times 40\,\text{mm}^2$. To validate the simulation results, the antenna parameters were measured. The results showed that the proposed antenna is capable of covering both the ISM frequency band (2.2–2.5 GHz) and UWB frequency band (3–26 GHz). This makes it suitable for various wireless communication applications requiring UWB and ISM frequencies, offering a promising solution.

1. INTRODUCTION

Antenna design has benefited from the use of metamaterials, which can improve antenna features like size, efficiency, gain, and bandwidth. These materials possess unique features, including negative dielectric constants, which are not found in nature. As a result, resonant antennas based on metamaterials have been extensively researched [1]. Multiband antennas are also attractive to researchers in academia and industry, as they can help create cheaper and smaller systems by cutting down the number of antennas needed. Ultra-wideband (UWB) technology is also appealing as it facilitates broadband communications with a very low energy radiation level, and UWB antennas have numerous applications [2, 3]. Hence, this paper presents an antenna that operates in both the UWB and ISM band, which can be used for various wireless communication applications.

Over the years, a plethora of multiband antennas have been proposed that are inspired or loaded with metamaterial structures. For instance, a dual-band antenna was introduced in [4], which is fed in coplanar waveguide (CPW) form. This antenna covers frequency bands ranging from 2.595 to 2.654 GHz and 3.185 to 4.245 GHz, utilizing split-ring resonator (SRR) and closed-ring resonator (CRR). Similarly, frequency bands for Bluetooth, GSM 1800, UMTS, DMB, and WIMAX were achieved by loading the antenna with several complementary metamaterial transmission line (CMTL) cells in [5]. A metamaterial-inspired antenna proposed in [6] covered four circularly polarized bands including 2.39–2.55 GHz, 3.05–3.1 GHz, 4–5 GHz, and 6.3–6.64 GHz. In [7], a multiband antenna inspired by metamaterials was proposed that covered different frequency bands ranging from 2.10 GHz to 6.5 GHz.

Received 7 June 2023, Accepted 25 July 2023, Scheduled 9 August 2023

* Corresponding author: Leila Ghanbari (leila.ghanbari@gmail.com).
The authors are with the Electrical Engineering Department, Faculty of Technical and Engineering, Imam Khomeini International University, Qazvin, Iran.

An L-shaped slot on the ground was used to simultaneously cover the WiMAX (3.5 GHz) and WLAN (5.8 GHz) frequency bands in a microstrip patch antenna with complementary split-ring resonator (CSRR) on the radiator element in [8]. Additionally, in [9], a dual-band antenna was presented that included UWB and Bluetooth. By adding a spiral to the UWB monopole antenna, the Bluetooth 2.45 GHz band was incorporated into its operation. Metamaterials can also be used to create band notches, as demonstrated in [10], where a monopole antenna loaded with CSRR was able to achieve a band-notch.

Metamaterial-inspired antennas have been the subject of numerous studies due to their ability to enhance antenna properties such as gain, bandwidth, and efficiency. In recent years, there has been significant interest in compact and wideband antennas that use metamaterial structures. For example, [11] investigated a single-polarized small patch antenna loaded with negative epsilon spiral lines, which operated in a wide frequency range of 2.38–2.95 GHz and provided omnidirectional radiation patterns. [12] explored the use of complementary split-ring resonators (CSRRs) and reactive impedance surface (RIS) to load a patch antenna. In addition, several compact patch antennas loaded with metamaterial structures have been proposed in [13–20]. These antennas have multiband performance, and some of them operate in the UWB range, providing a low-energy radiation level and broad communication capabilities.

The proposed antenna design presents a significant contribution to the field of antenna design, as it achieves dual-band performance covering both UWB and ISM band, which is not commonly seen in previous studies. Moreover, the use of SRR as a loading element to the main radiator patch is a unique approach that enhances the antenna's performance by generating multiple new resonance frequencies, as demonstrated by the CMA analysis. The use of an FR4 substrate in the fabrication process makes the antenna more accessible and cost-effective to produce. The measured results showing good agreement with the simulated ones which indicates that the proposed design is promising and can potentially be utilized in various applications requiring dual-band and wideband antenna performance.

2. ANALYSIS OF ANTENNA CHARACTERISTIC MODES

2.1. Characteristic Mode Theory

Characteristic Mode Theory (CMA) has gained significant attention in the field of antenna engineering as it allows for the determination of resonance modes for antennas with arbitrary shapes [2]. This method is especially helpful because it allows the obtainment of modes that do not depend on feeding networks. The process of utilizing CMA involves obtaining an impedance matrix, using the method of moments based on the radiating structure. Next, a generalized eigenvalue equation is established, and by solving this equation, the characteristic current modes are obtained. If we consider the impedance matrix Z, as defined in Equation (1) where R and X represent the real and imaginary parts of Z respectively, we can obtain the characteristic modes using the generalized eigenvalue Equation (2).

$$Z = R + jX \tag{1}$$

$$X(J_n) = \lambda_n R(J_n) \tag{2}$$

Symbol λ_n represents the eigenvalue, while J_n corresponds to the eigenvectors or eigen-currents [21]. The total current on the antenna can be represented as a weighted sum of the characteristic current modes using the following equation [22].

$$J = \sum\nolimits_n \beta_n J_n \tag{3}$$

To evaluate characteristic modes, simulation was carried out using CST software, which involved examining the characteristic angle β_n and modal significance MS_n. A brief physical interpretation of these modes was provided in [23], which suggests that modes with β close to 180 degrees radiate, while modes close to 90 or 270 degrees store energy. By exciting the desired modes, the antenna can achieve the desired frequency response.

$$\beta_n = 180^\circ - \tan^{-1}(\lambda_n) \tag{4}$$

$$MS_n = 1/(1 + J\lambda_n) \tag{5}$$

2.2. Modal Analysis

To gain insight into the radiation mechanism of the proposed antenna, we analyzed the first six resonant modes. We compared the characteristic modes of two different structures: the conventional circular patch and the proposed structure (shown in Figure 1), to investigate the effect of the radiating patch shape. It is important to note that the modes obtained through characteristic mode analysis depend

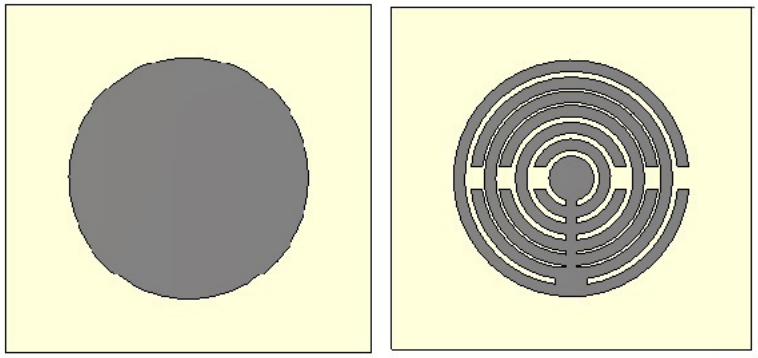

Figure 1. (a) Conventional circular radiating structure. (b) Proposed structure.

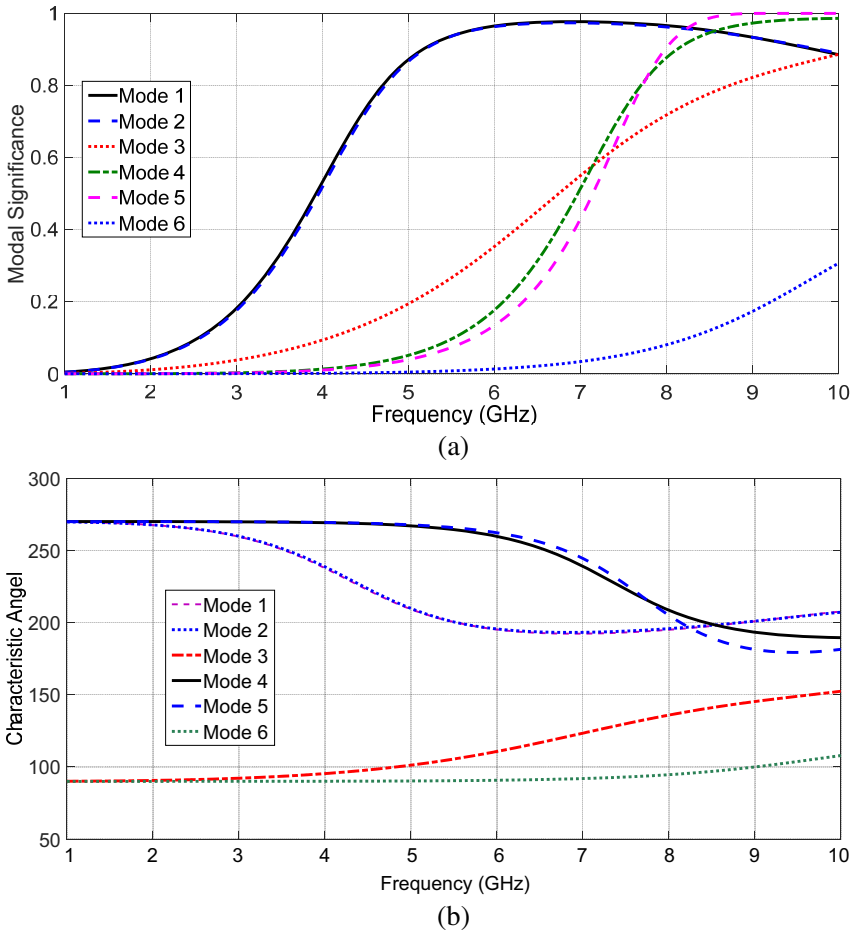

Figure 2. (a) Modal significance, and (b) characteristic angle of the conventional circular radiating structure with a radius of 10.5 mm.

solely on the patch's structure and are independent of the feeding and ground plane. The modal significance and characteristic angle of the first six modes for the circular patch structure on a 1.6 mm thick FR4 substrate are illustrated in Figure 2. Based on the simulation results, it is evident that this structure can achieve a high level of broadband. At around 4.4 GHz, modes 1 and 2 can begin radiating at a characteristic angle of approximately 225 degrees. Previous works have demonstrated antennas based on this patch [2, 3]. Figure 3 shows the modal currents, indicating that mode 1 and

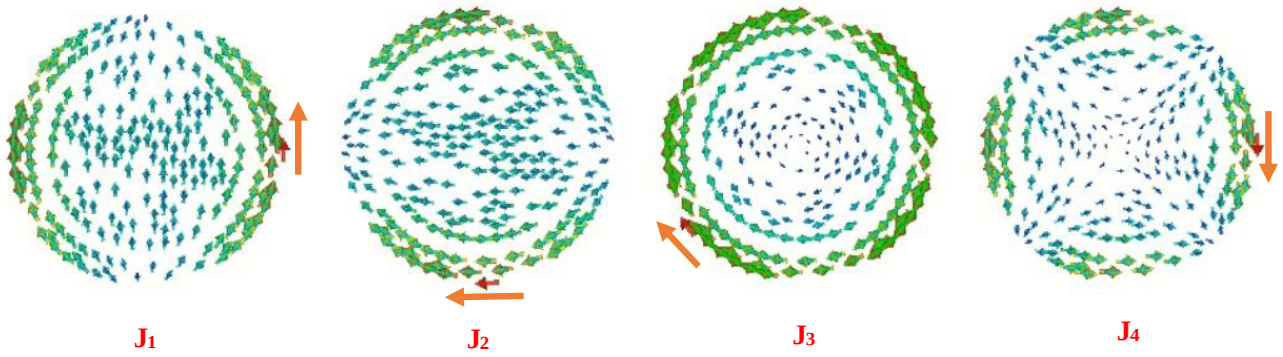

Figure 3. Surface current distribution of first four modes at 6 GHz.

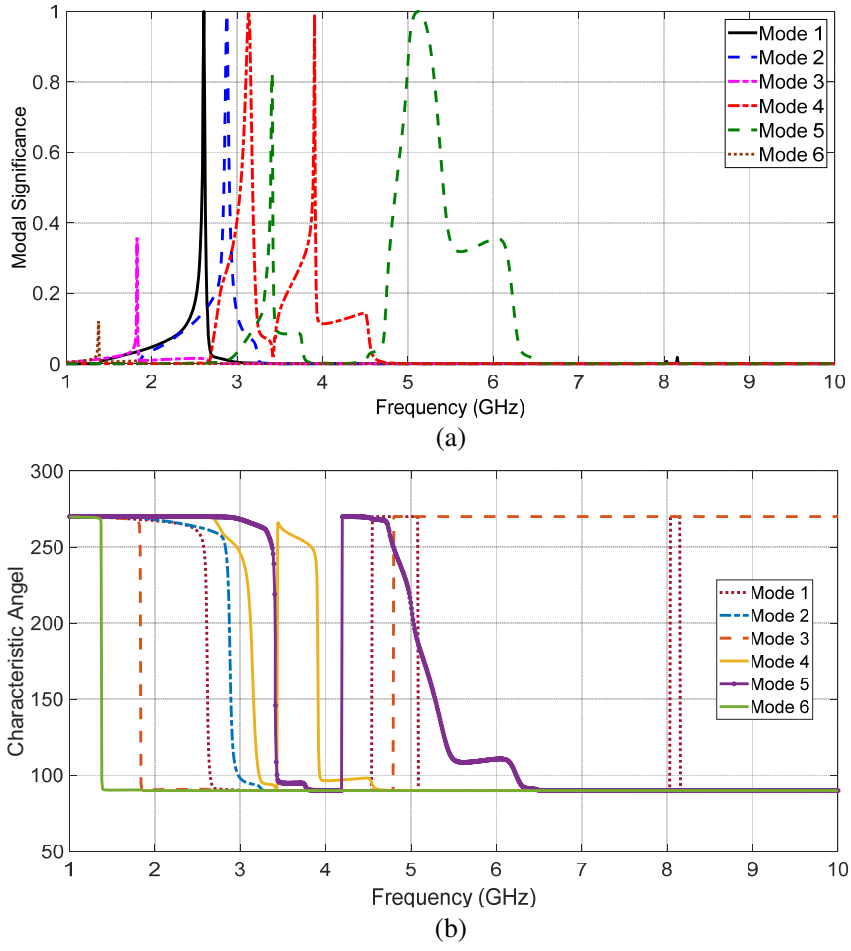

Figure 4. (a) Modal significance and (b) characteristic angle of the proposed structure inspired by metamaterials.

mode 2 are perpendicular to each other, but have no phase differences. We modified the circular patch structure, taking inspiration from metamaterials (as shown in Figure 4) to create numerous radiation modes, with a new resonant frequency appearing at 2.5 GHz. Properly exciting this mode can lead to an improvement in the circular antenna's bandwidth, allowing it to cover the ISM band. The modal currents for the first four modes are shown in Figure 5. The dimensions of the modified patch can be found in Table 1.

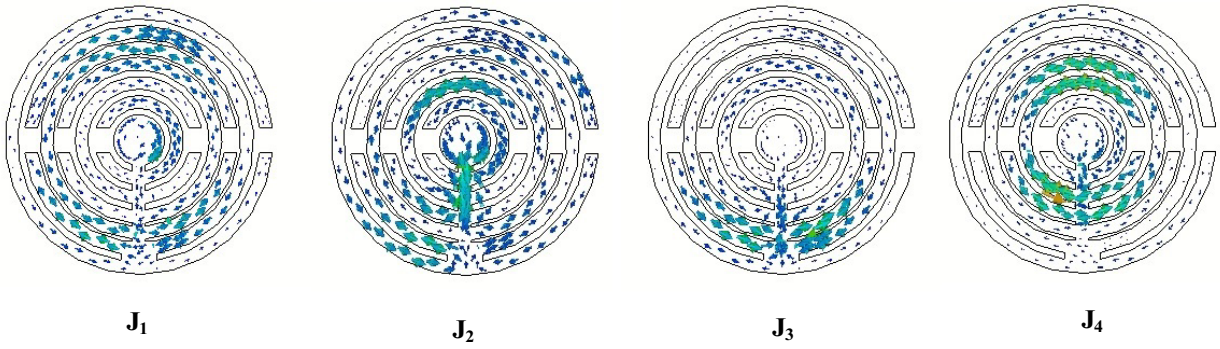

Figure 5. Surface current distribution of first four modes at 6 GHz.

Table 1. The proposed antenna dimensions.

Parameter	Value (mm)	Parameter	Value (mm)
L	38	W	40
Wn	3	Ln	3
h	1.75	Lg	12
$d1$	0.75	$d2$	0.5
Rn	10		

3. DESIGN AND ANALYSIS OF ANTENNA INSPIRED BY METAMATERIALS

The antenna design shown in Figure 6 consists of a monopole inspired by metamaterials and a ground plane. The antenna was fabricated and simulated on an FR4 substrate with a thickness of 1.6 mm and a relative dielectric constant of 4.4. The antenna has a width of W and a length of L, and it is connected to a 50-ohm microstrip line with a width of WF. The dimensions of the modified ground plane are $W \times Lg$, and a slot with dimensions $Ln \times Wn$ is located below the feed line to improve impedance matching. The corners of the ground plane are truncated at a radius of Rn. The distance between the central circular patch and the nearest SRR is $d1$, and the other SRRs are spaced at intervals of $d2$. The distance between the radiating element and the ground is represented by $h(LF - Lg)$. High Frequency Structure Simulator (HFSS) and CST Microwave Studio were used for simulation to investigate the proposed antenna's performance. As seen in the characteristic mode analysis section, placing a metamaterial slot created a new band at 2.5 GHz. Also, since the proposed structure has numerous radiating modes, it can have a high bandwidth. The simulation results, presented in Figure 7, show that the reflection coefficient is better than -20 dB at a frequency of 2.4 GHz and better than -13 dB from 3.1 to 26 GHz. Table 1 displays the antenna dimensions.

To evaluate the impact of incorporating the SRR in the proposed antenna, the conventional monopole antenna was also simulated using CST. The comparison between the reflection coefficients of both antennas is illustrated in Figure 8. It can be observed that the first resonant frequency of the simple circular antenna closely aligns with a quarter wavelength [24]. While the resonant frequencies of the proposed antenna, particularly at higher frequencies beyond 12 GHz, bear a close resemblance to

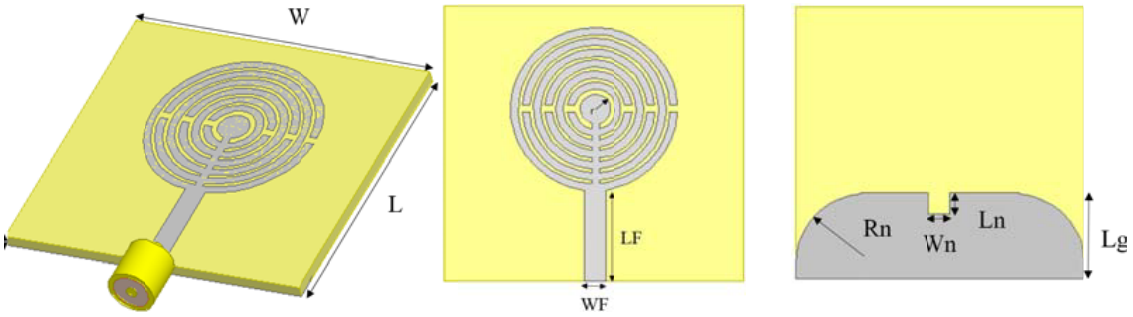

Figure 6. Proposed antenna showing: (a) Three-dimensional shape of the antenna on FR4 substrate, (b) radiating element fed by microstrip, (c) modified ground plane.

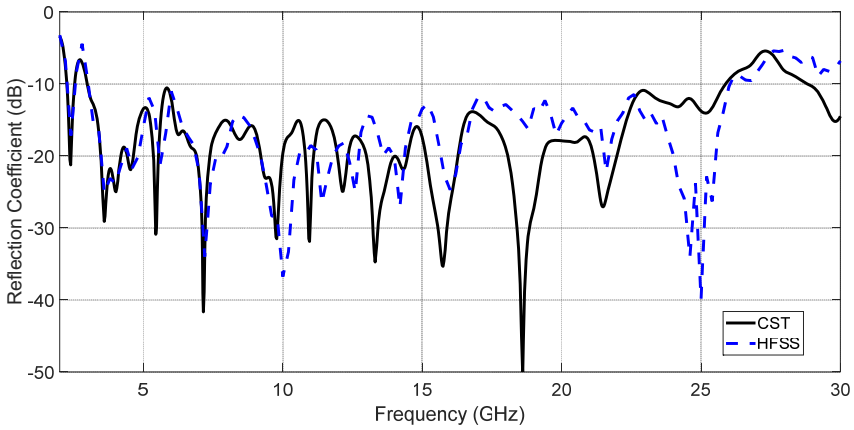

Figure 7. Simulated reflection coefficient using HFSS and CST.

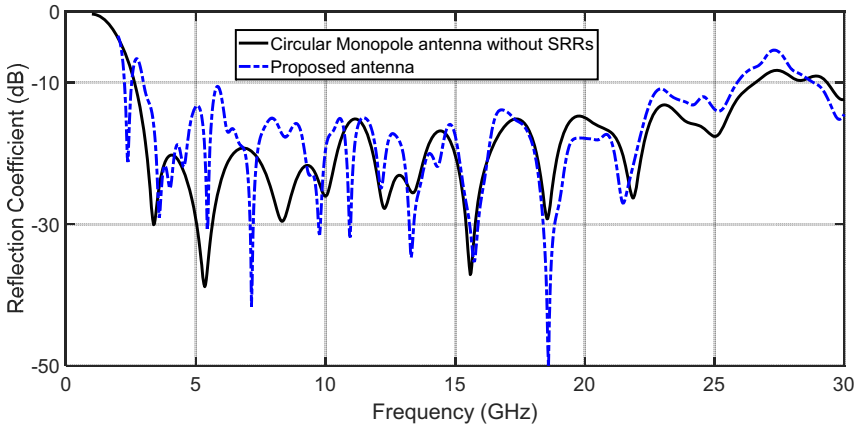

Figure 8. Comparison of reflection coefficients between a simple circular monopole antenna and the proposed antenna with similar dimensions.

those of the simple circular antenna. There are additional resonant frequencies, particularly at 2.4 GHz. This novel approach, which has not been employed previously, represents a new contribution and is presented in this paper.

The proposed antenna is designed to operate in two frequency bands, covering the ISM band and

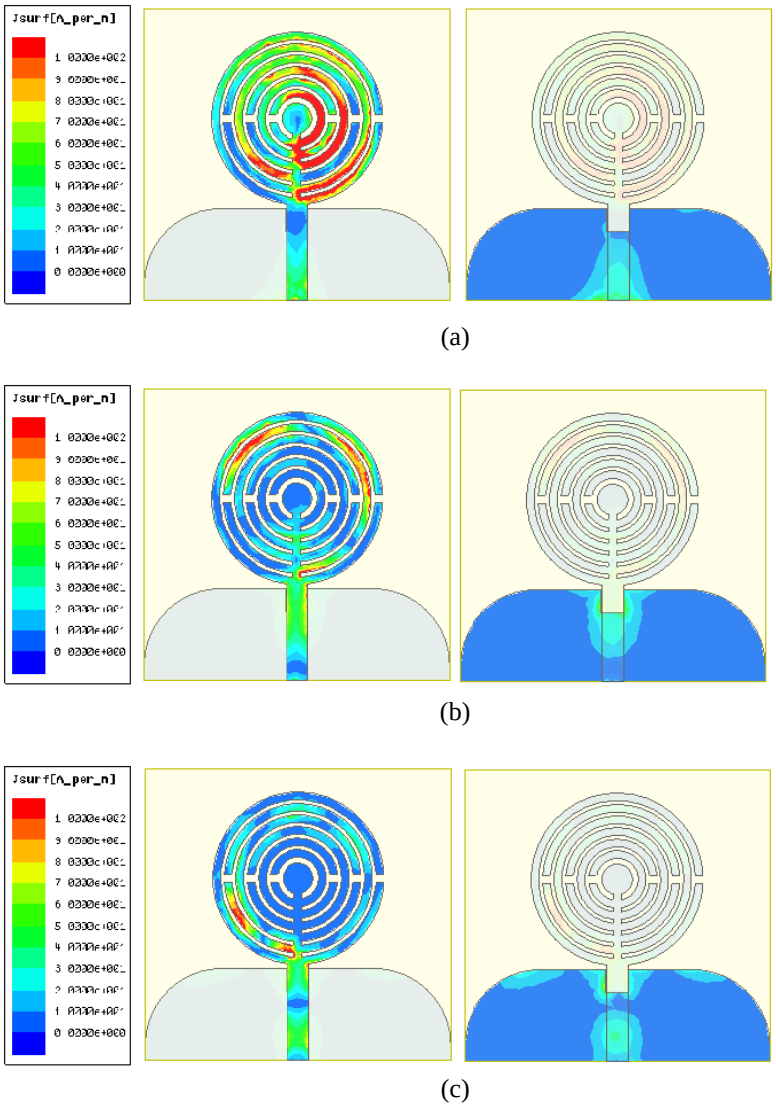

Figure 9. Current distribution on the ground plane and radiator at frequencies (a) 2.4 GHz, (b) 5.7 GHz, (c) 9.6 GHz.

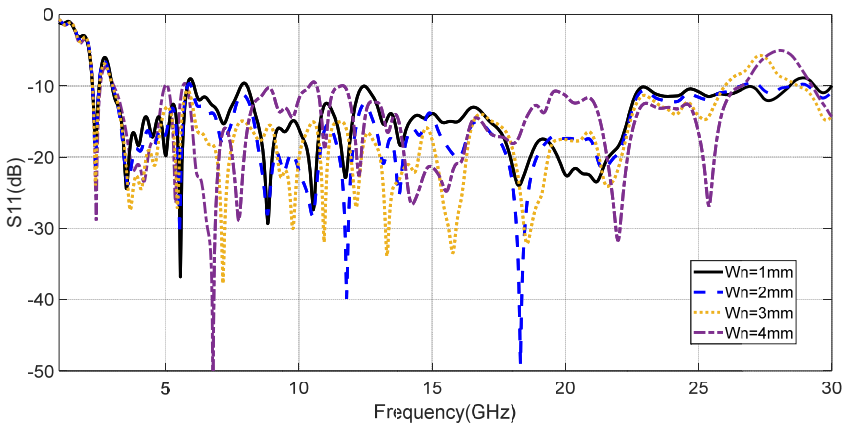

Figure 10. Variation of reflection coefficient with respect to the change of Wn ($Wn = Ln$).

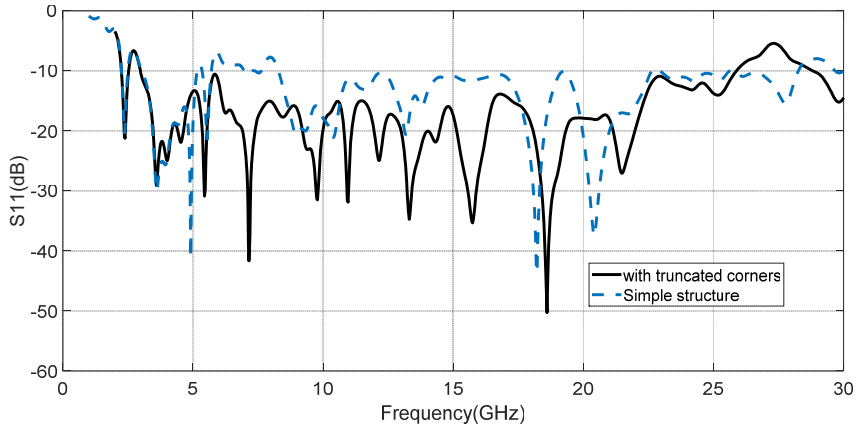

Figure 11. Comparison of reflection coefficient in a simple rectangular ground plane antenna and a ground plane with rounded corners.

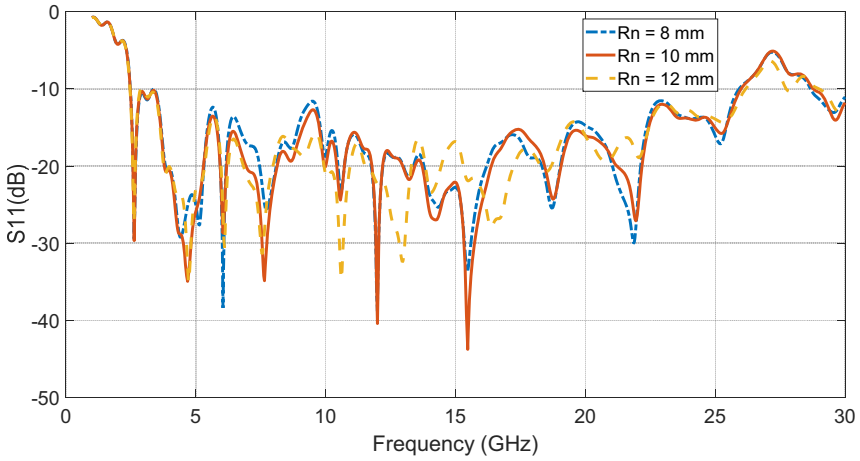

Figure 12. Relationship between changes in the reflection coefficient and variations in the truncation radius Rn.

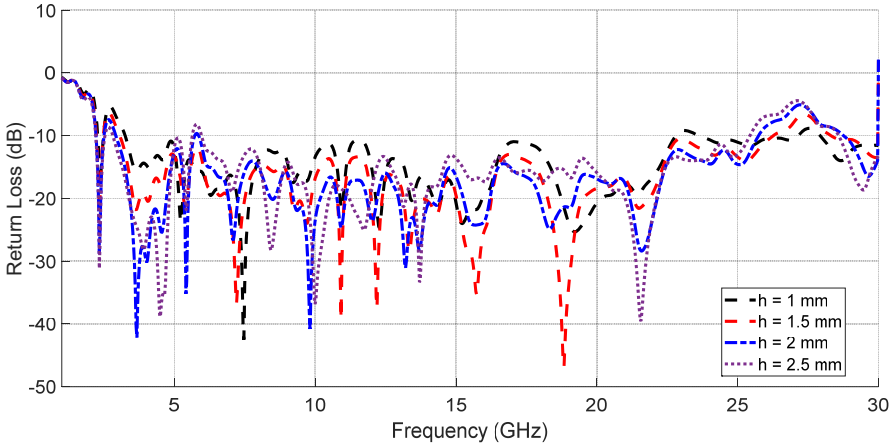

Figure 13. Relationship between changes in the reflection coefficient and variations in the distance between the radiating element and the ground plane (h).

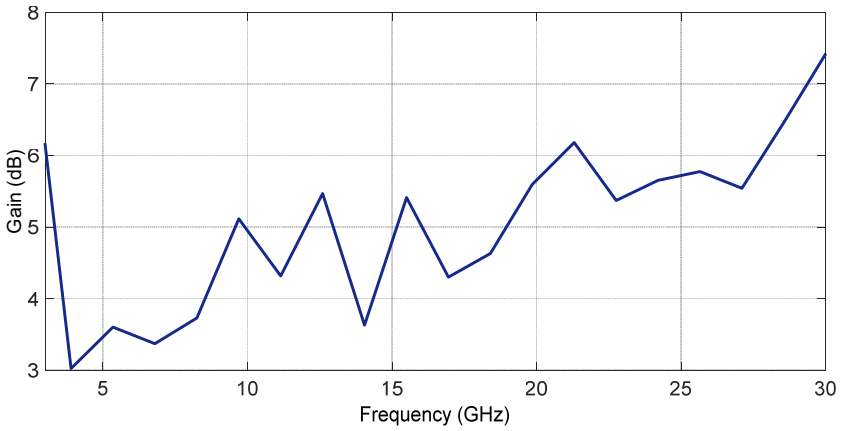

Figure 14. Maximum gain of the proposed antenna over frequency.

UWB. Figure 9 depicts the simulated current distribution of the antenna at 2.4 GHz, 5.7 GHz, and 9.6 GHz. At 2.4 GHz, the current distribution is concentrated on the edges of the SRRs, while on the ground plane, the concentration is higher on its edges. To achieve better impedance matching, the rectangular ground plate has been modified as shown. Figure 10 demonstrates the effect of changing the dimensions of the slot (Wn and Ln) on the reflection coefficient. Furthermore, Figure 11 illustrates the impact of rounding the corners of the ground plane, especially for frequencies above 5 GHz, and this slot improves impedance matching. Variation of Rn is indicated in Figure 12. The distance between the radiating element and the ground plane is another important parameter affecting the reflection

Table 2. Comparison with related references.

Ref	Structure	Bandwidth		polarization	Dimension		substrate
		Frequency (GHz)	%		mm × mm × mm	$\lambda_0 \times \lambda_0 \times \lambda_0$	
[6]	monopole	2.39–2.55 3.05–3.1 4–5 GHz 6.3–6.64	6.4 1.6 22 5.2	circular	32 × 38 × 1.6	0.25 × 0.28 × 0.01 ($\lambda_0 = 125$ mm)	FR4
[4]	monopole	2.595–2.654 3.185–4.245	2.2 28	NA	31.7 × 27 × 1.6	0.27 × 0.23 × 0.01 ($\lambda_0 = 115$ mm)	FR4
[7]	monopole	1.98–2.48 2.83–3.00 3.46–3.71 4.08–4.59 5.44–5.67 6.40–7.66	22 5.8 6.9 11.7 4 18	NA	40 × 40 × 0.8	0.28 × 0.28 × 0.005 ($\lambda_0 = 142$ mm)	FR4
[8]	monopole	3.4–3.6 5.7–5.9	5.7 3.4	NA	40 × 25 × 1.524	0.47 × 0.29 × 0.02 ($\lambda_0 = 85$ mm)	Neltec NH9332
[9]	monopole	2.45 3.3–3.6 5.15–5.35 5.725–5.825 8	8.6 3.8 1.7	NA	24 × 17 × 0.787	0.19 × 0.13 × 0.006 ($\lambda_0 = 122$ mm)	Duriod 5880
This work	monopole	2.2–2.5 3–26	12 158	linear	38 × 40 × 1.6	0.27 × 0.29 × 0.01 ($\lambda_0 = 136$ mm)	FR4

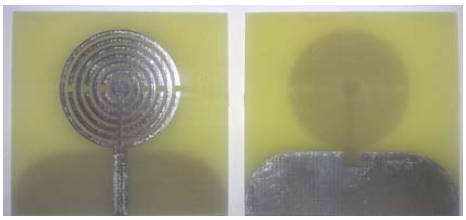

(a)

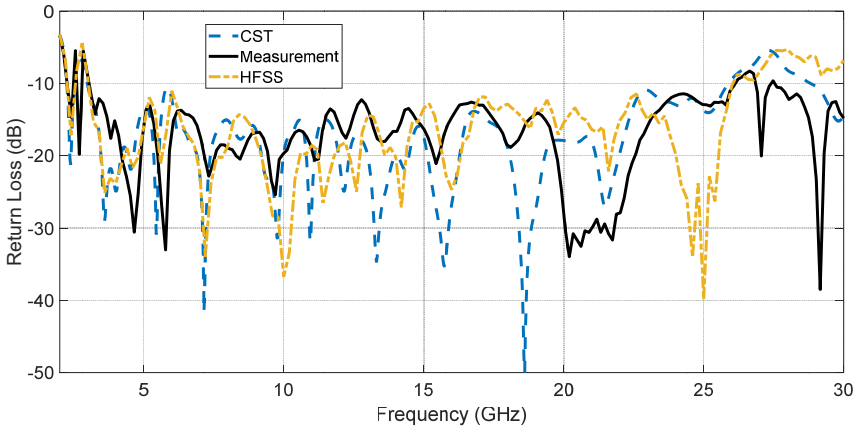

(b)

Figure 15. (a) Fabricated proposed antenna sample, (b) comparison of simulated and measured reflection coefficient.

coefficient, as shown in Figure 13. The simulated maximum gain is indicated in Figure 14.

The antenna was constructed on a 1.6 mm thick FR4 substrate with a dielectric constant of 4.4, and its characteristics were evaluated. Figure 15 compares the simulated and measured reflection coefficients, demonstrating that the antenna effectively spans the UWB and ISM band. The radiation patterns were measured at 2.4 GHz and 5.7 GHz and compared to simulation results. The normalized radiation patterns in decibels are shown in Figure 16. The antenna's radiation patterns are omnidirectional with linear polarization, as shown by these results.

In the literature, the proposed metamaterial-inspired antenna was compared to previously introduced antennas, and the results are presented in Table 2. This antenna boasts a broader bandwidth than its references, covering the ranges of 2.2–2.5 GHz and 3–26 GHz. Additionally, the antenna's linear polarization contributes to its overall performance.

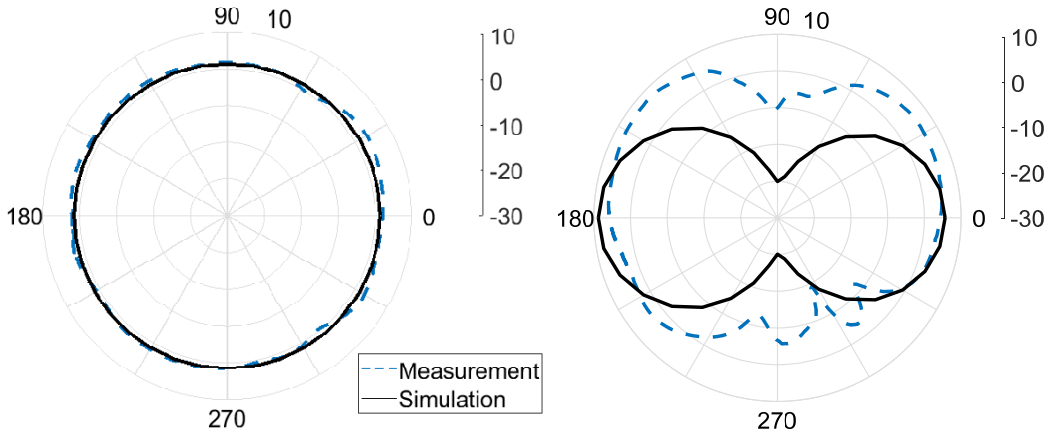

(a)

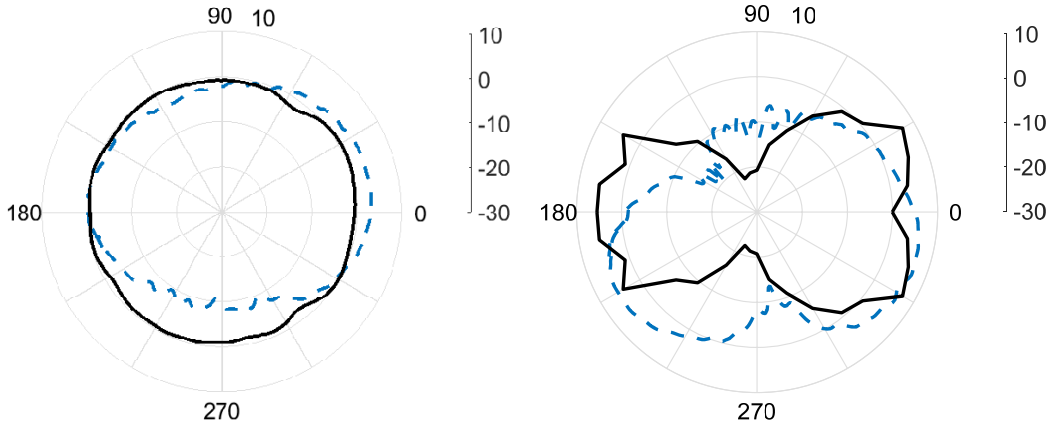

(b)

Figure 16. Measured and simulated radiation patterns (dashed line: measurement) in E-plane and H-plane at (a) 2.4 GHz and (b) 5 GHz in decibels.

4. CONCLUSION

This paper proposes a dual-band monopole antenna inspired by metamaterials, which exhibits excellent reflection coefficients. Specifically, it achieves a reflection coefficient better than −20 dB within the frequency band of 2.2–2.5 GHz and a reflection coefficient better than −13 dB in the frequency range of 3.1–26 GHz. This enables the antenna to operate in both the ISM band and UWB. Characteristic Mode Analysis (CMA) has been used for the survey of the proposed antenna. The results indicate that the metamaterial-inspired design has more resonance frequencies than a conventional circular monopole antenna. We introduced SRRs on the patch antenna, which created a new resonance frequency at 2.4 GHz. Moreover, we modify the ground plane to achieve better impedance matching. The proposed antenna has omnidirectional radiation patterns, and its dimensions are $38 \times 40\,\text{mm}^2$. We fabricated the antenna on an FR4 substrate and measured its parameters. The measurement results matched well with the simulation ones, indicating that it is suitable for wireless applications.

CONFLICT OF INTEREST STATEMENT

The author declares that there are no conflicts of interest.

REFERENCES

1. Marqués, R., F. Martin, and M. Sorolla, *Metamaterials with Negative Parameters: Theory, Design, and Microwave Applications*, John Wiley & Sons, 2011.
2. Ghanbari, L., A. Keshtkar, S. Ghanbari, and S. Jarchi, "Planar low VSWR monopole antenna for UWB and LTE communication," *2016 16th Mediterranean Microwave Symposium (MMS)*, 1–4, IEEE, 2016.
3. Ghanbari, L., S. Nikmehr, and M. Rezvani, "A novel small UWB antenna using new fractal-like geometry," *2011 IEEE Applied Electromagnetics Conference (AEMC)*, 1–4, IEEE, 2011.
4. Si, L.-M., W. Zhu, and H.-J. Sun, "A compact, planar, and CPW-fed metamaterial-inspired dual-band antenna," *IEEE Antennas and Wireless Propagation Letters*, Vol. 12, 305–308, 2013.
5. Xu, H.-X., G.-M. Wang, Y.-Y. Lv, M.-Q. Qi, X. Gao, and S. Ge, "Multifrequency monopole antennas by loading metamaterial transmission lines with dual-shunt branch circuit," *Progress In Electromagnetics Research*, Vol. 137, 703–725, 2013.

6. Rao, M. V., B. Madhav, T. Anilkumar, and B. P. Nadh, "Metamaterial inspired quad band circularly polarized antenna for WLAN/ISM/Bluetooth/WiMAX and satellite communication applications," *AEU-International Journal of Electronics and Communications*, Vol. 97, 229–241, 2018.
7. Selvi, N. T., P. T. Selvan, S. Babu, and R. Pandeeswari, "Multiband metamaterial-inspired antenna using split ring resonator," *Computers & Electrical Engineering*, Vol. 84, 106613, 2020.
8. Malik, J. and M. Kartikeyan, "Metamaterial inspired patch antenna with L-shape slot loaded ground plane for dual band (WiMAX/WLAN) applications," *Progress In Electromagnetics Research Letters*, Vol. 31, 35–43, 2012.
9. Reddy, G. S., A. Kamma, S. K. Mishra, and J. Mukherjee, "Compact bluetooth/UWB dual-band planar antenna with quadruple band-notch characteristics," *IEEE Antennas and Wireless Propagation Letters*, Vol. 13, 872–875, 2014.
10. Li, W. T., Y. Q. Hei, W. Feng, and X. W. Shi, "Planar antenna for 3G/Bluetooth/WiMAX and UWB applications with dual band-notched characteristics," *IEEE Antennas and Wireless Propagation Letters*, Vol. 11, 61–64, 2012.
11. Liu, L.-Y. and B.-Z. Wang, "A broadband and electrically small planar monopole employing metamaterial transmission line," *IEEE Antennas and Wireless Propagation Letters*, Vol. 14, 1018–1021, 2015.
12. Dong, Y., H. Toyao, and T. Itoh, "Design and characterization of miniaturized patch antennas loaded with complementary split-ring resonators," *IEEE Transactions on Antennas and Propagation*, Vol. 60, No. 2, 772–785, 2011.
13. Wan, Y. T., D. Yu, F. S. Zhang, and F. Zhang, "Miniature multi-band monopole antenna using spiral ring resonators for radiation pattern characteristics improvement," *Electronics Letters*, Vol. 49, No. 6, 382–384, 2013.
14. Amani, N., M. Kamyab, A. Jafargholi, A. Hosseinbeig, and J. Meiguni, "Compact tri-band metamaterial-inspired antenna based on CRLH resonant structures," *Electronics Letters*, Vol. 50, No. 12, 847–848, 2014.
15. Pandey, G., H. Singh, P. Bharti, and M. Meshram, "Metamaterial-based UWB antenna," *Electronics Letters*, Vol. 50, No. 18, 1266–1268, 2014.
16. Sarkar, D., K. Saurav, and K. V. Srivastava, "Multi-band microstrip-fed slot antenna loaded with split-ring resonator," *Electronics Letters*, Vol. 50, No. 21, 1498–1500, 2014.
17. Nordin, M. A. W., M. T. Islam, and N. Misran, "Design of a compact ultrawideband metamaterial antenna based on the modified split-ring resonator and capacitively loaded strips unit cell," *Progress In Electromagnetics Research*, Vol. 136, 157–173, 2013.
18. Soliman, A., D. Elsheakh, E. Abdallah, and H. El-Hennawy, "Multiband printed metamaterial inverted-F antenna (IFA) for USB applications," *IEEE Antennas and Wireless Propagation Letters*, Vol. 14, 297–300, 2014.
19. Majedi, M. S. and A. R. Attari, "A compact and broadband metamaterial-inspired antenna," *IEEE Antennas and Wireless Propagation Letters*, Vol. 12, 345–348, 2013.
20. Islam, M., M. T. Islam, M. Samsuzzaman, and M. R. I. Faruque, "Compact metamaterial antenna for UWB applications," *Electronics Letters*, Vol. 51, No. 16, 1222–1224, 2015.
21. Chen, Y. and C.-F. Wang, *Characteristic Modes: Theory and Applications in Antenna Engineering*, John Wiley & Sons, 2015.
22. Saurav, K., D. Sarkar, and K. V. Srivastava, "Dual-polarized dual-band patch antenna loaded with modified mushroom unit cell," *IEEE Antennas and Wireless Propagation Letters*, Vol. 13, 1357–1360, 2014.
23. Garbacz, R. and R. Turpin, "A generalized expansion for radiated and scattered fields," *IEEE Transactions on Antennas and Propagation*, Vol. 19, No. 3, 348–358, 1971.
24. Liang, J., C. C. Chiau, X. Chen, and C. G. Parini, "Study of a printed circular disc monopole antenna for UWB systems," *IEEE Transactions on Antennas and Propagation*, Vol. 53, No. 11, 3500–3504, 2005.